ELSEVIER

Journal of Chromatography A, 672 (1994) 1–10

JOURNAL OF CHROMATOGRAPHY A

Modeling of radial heterogeneity in chromatographic columns Columns with cylindrical symmetry and ideal model☆

Tong Yun[a], Georges Guiochon*[,b]

[a]*Department of Chemical Engineering, University of Tennessee, Knoxville, TN 37996-1503, USA and Division of Analytical Chemistry, Oak Ridge National Laboratory, Oak Ridge, TN 37831-6120, USA*

[b]*Department of Chemistry, University of Tennessee, Knoxville, TN 37996-1503, USA and Division of Analytical Chemistry, Oak Ridge National Laboratory, Oak Ridge, TN 37831-6120, USA*

(First received December 6th, 1993; revised manuscript received February 11th, 1994)

Abstract

Elution band profiles are calculated for radially heterogeneous cylindrical columns, assuming an infinite rate of mass transfer kinetics and no axial dispersion. Steady-state flow-rate is assumed, with a given, cylindrical radial distribution of the velocity. Parabolic, cuspal and cosinusoidal distributions were studied, all three with either the velocity maximum or minimum in the column center. In all cases, strong changes in the band profiles appear for velocity distributions in which the ratio of the maximum to the minimum velocity is as low as 1.05. Some of the profiles obtained appear to be similar to experimental profiles.

1. Introduction

The theory of chromatography has always assumed so far that the column is radially homogeneous, that the feed is evenly spread over the entire column cross-section and that plug flow is achieved throughout the column [1–5]. Accordingly, the mass balance equation is written and solved in a single space dimension, and the mathematical problem studied has only two dimensions, the column length and the time. However, even analytical chromatographic columns are not homogeneous. There are a few scattered reports in the literature showing significant variations of the mobile phase velocity across the column cross-section, probably caused by a lack of homogeneity of the packing density [6–8]. Preliminary results [9] obtained in our laboratory lead to the same conclusion.

Analytical columns are typically 0.46 cm I.D. and 10–30 cm long, so they are 20 to 60 times longer than they are wide. Even in this case, Knox and Parcher [10] have shown that trans-column equilibration is a comparatively slow process, much slower than axial migration. So, in practice, most sample molecules injected in the center of the column never come close to the column wall. In such a case, radial diffusion cannot even out the effects of fluctuations of the column characteristics related to an inhomogeneous packing density, if these fluctuations take place over a distance significant compared to the column radius. Column heterogeneity causes

* Corresponding author. Address for correspondence: Department of Chemistry, University of Tennessee, Knoxville, TN 37996-1503, USA.

☆ Presented at the *22nd Annual Meeting of the Spanish Chromatography Group, Barcelona, October 20–22, 1993.*

0021-9673/94/$07.00
SSDI 0021-9673(94)00144-X

local fluctuations of the external porosity, the permeability, and the retention factors. It probably explains a large part of the plate height contribution attributed to eddy diffusion [11].

If even an analytical column cannot be considered as homogeneous, a preparative column, typically several inches to a few feet in diameter, and rarely more than 2 or 3 ft. (1 in. = 2.54 cm, 1 ft. = 30.48 cm) long, certainly cannot. Accounting for the local fluctuations in the packing density becomes necessary. This problem has been identified by Giddings [12] long ago. Its solution does not raise major difficulties of principle, but requires the answers to a number of practical problems. The straightforward solution would be to write and solve the mass balance equation of chromatography in a three-dimension space, but this would require an enormous amount of computing power, even though the number of meshes needed in the grid would be much smaller in the two radial directions than along the column axis. Furthermore, the solution of this problem requires the definition of proper boundary conditions, *i.e.*, of the distribution of the packing heterogeneity, a parameter which is usually not available. Finally, experiments show that the efficiency of wide-bore preparative columns is not much below that of analytical columns packed with the same stationary phase. The influence of the column heterogeneity on the profile of large-size samples cannot be important when the profiles obtained with preparative columns remain close to those observed for analytical columns operated at the same loading factor. Thus, a simple correction would be useful in most cases. The general problem does not have to be solved at this stage.

Preparative columns are cylindrical. The lack of stability of the packing observed in numerous cases, the formation of important voids at the top of the bed after operating times ranging from a few days to a few weeks have been attributed by their operators to the lack of bed support by the column wall [13,14]. This suggests that if the bed is heterogeneous, the first approximation for a distribution of the packing density should be cylindrical. Indeed, a cylindrical distribution of the mobile phase velocity in analytical [6–8] or narrow-bore columns [9] is in agreement with experimental results. The long-term stability of the packing bed requires a form of dynamic compression. A number of axial and radial compression columns are currently in use. Because of its geometry, the radial compression columns must be cylindrical with a good degree of approximation. Accordingly, the study of the behavior of band profiles under linear and non-linear conditions in cylindrical, heterogeneous columns would be a satisfactory approximation, and the solution of the chromatographic problem in this case would give an excellent idea of the degree to which column heterogeneity can affect the performance of preparative columns. The advantage of this approach is to reduce the problem to a two-space dimension one, decreasing considerably in the process the amount of computing power required for the calculation of numerical solutions.

If we assume a cylindrical symmetry for the column, the packing is not homogeneous in the radial direction, but the distribution profile is the same in all planes passing through the column axis. As a consequence, the packing density, the column external porosity, and its permeability are constant along any parallel to the column axis. Hence, the mobile phase velocity will be everywhere parallel to the column axis and constant along a parallel to this axis. Because chromatographic columns are always used after proper equilibration between the stationary and the mobile phases, we do not need to solve a time-dependent hydraulic equation. It is legitimate to assume a stable cylindrical distribution of the mobile phase velocity, related to the permeability distribution, and to consider the distribution of the mobile phase velocity as a part of the boundary conditions.

The simplest model of non-linear chromatography is the ideal model. In this model, constant equilibrium of the studied component between the stationary and the mobile phase is assumed. Furthermore, the axial dispersion, due to molecular diffusion and to eddy dispersion is neglected. A linear column operated with these assumptions would have an infinite efficiency. A third assumption of the ideal model is plug flow

distribution. In this work, we investigate what happens if this third assumption is relaxed. We study the band profiles observed in a column where axial and radial dispersion are neglected, and where local phase equilibrium is reached constantly, but where there is a cylindrical distribution of the mobile phase velocity.

2. Theory

In this work, we assumed that the column has an infinite efficiency and that the equilibrium isotherm is given by the Langmuir equation. We divide the column in an infinite number of concentric annular columns of thickness d_r and radius r between 0 and R_c, the column radius. The velocity is constant in each of these annular columns, so its contribution to the elution profile is derived by applying the solution of the ideal model. The elution profiles of the sample on each column are identical, but their breakthrough times are shifted since the velocity varies from annular column to annular column. Summation of these individual contributions over the column radius will give the elution profile as recorded by a conventional detector. It will be possible also to represent the elution of isoconcentration surfaces in order to illustrate the propagation of the zones. We discuss successively the elution profile of the ideal model in the case of the Langmuir isotherm, the velocity profiles selected and the derivation of the profiles.

2.1. The ideal model of chromatography

The ideal model assumes a linear column with an infinite efficiency. In this case the mass balance of a compound is written

$$\frac{\partial C}{\partial t} + F \cdot \frac{\partial q}{\partial t} + u(r) \cdot \frac{\partial C}{\partial z} = 0 \tag{1}$$

where C and q are the local concentrations in the mobile and stationary phases, respectively, F is the phase ratio [$F = (1 - \epsilon)/\epsilon$, with ϵ total column porosity], and $u(r)$ is the mobile phase velocity. Since we assume constant equilibrium between the two phases, q and C are related by the equilibrium isotherm, and given by the Langmuir equation

$$q = \mathrm{f}(C) = \frac{aC}{1 + bC} \tag{2}$$

where a and b are numerical coefficients characterizing the compound studied and the stationary phase. The local concentrations C and q are functions of the two spacial coordinates, z and r and of time, t: $C = C(z,r,t)$. The initial condition is

$$C(z, r, t = 0) = 0 \tag{3}$$

indicating that at time $t = 0$, the column is equilibrated with the pure mobile phase. The boundary condition is the injection of a rectangular concentration pulse of width t_p and height C_0

$$C(z = 0,r,t) = C_0 \text{ for } 0 < t \leq t_p \tag{4a}$$

$$C(z = 0,r,t) = 0 \text{ for } t_p < t \tag{4b}$$

Wilson [15] and DeVault [1] have shown that, for a convex upwards isotherm such as the Langmuir model, the elution profile has two different sides, a front shock and a rear diffuse boundary [16]. This phenomenon arises from the fact that, in the ideal model, a velocity can be associated to each concentration. Thus, if we consider a linear (*i.e.*, homogeneous) column, any concentration propagates along a straight line in the z,t space (z = column length, t = time). The rear, diffuse profile is given by the equation

$$t(r,C) = t_p + t_0(r)\left(1 + F \cdot \frac{dq}{dC}\right) \tag{5a}$$

$$= t_p + t_0(r)\left(1 + \frac{aF}{(1 + bC)^2}\right) \tag{5b}$$

where $t_0(r)$ is the hold-up time, now function of the radial position [$t_0(r) = L/u(r)$, where L is the column length], and $t(r, C)$ is the retention time of the concentration C along the cylinder of radius r coaxial with the column. Eq. 5a applies to any isotherm, and Eq. 5b to the Langmuir model. The profiles end with the elution of the concentration 0, at time

$$t_R(r, C = 0) = t_p + t_0(1 + aF) = t_p + t_{R,0}(r) \quad (5c)$$

with $aF = k'_0$, the classical retention factor under linear conditions. The retention time of the concentration shock is also the retention time of the band maximum. In the case of a Langmuir isotherm, it is given by [5,16]

$$t_R(r) = t_p + t_0(r) + [t_{R,0}(r) - t_0(r)]\left(1 - \sqrt{L_f}\right)^2 \quad (6)$$

where L_f is the loading factor or ratio of the sample size to the sample amount needed to saturate the column. This column saturation capacity is proportional to the amount of stationary phase in the column and to the ratio a/b of the two coefficients of the Langmuir isotherm. The maximum concentration of the local elution profile is

$$C_M = \frac{\sqrt{L_f}}{b(1 - \sqrt{L_f})} \quad (7)$$

It is independent of the radial position, but this maximum concentration is eluted at time $t_R(C_M, r)$, which depends on r.

2.2. Velocity distribution

The exact distribution of the mobile phase velocity across the column is extremely complicated. It reflects the complexity of the packing structure. The velocity is 0 inside each particle and along its surface. Between particles, it raises very rapidly from the particle surface to the core of the channels, with rapid fluctuations in direction and intensity, as it is probable that more or less stable eddies take place inside some of the minute holes between particles. Any tractable model must simplify drastically the actual flow-rate distribution by considering averages.

The simplest model is the one currently used, the velocity is averaged over the entire column cross-section area by dividing the flow-rate by either πR_c^2 or by the actual cross-section area available to the stream, $\pi\epsilon_e R_c^2$, with ϵ_e the external porosity (approaches favored in hydraulics), or by the cross-section area of the column available to the mobile phase, $\pi\epsilon R_c^2$ (approach favored by chromatographers when they consider the mobile phase flow velocity, $u = L/t_0$). It is legitimate to average out the local fluctuations of the mobile phase velocity over short distances because dispersion may smooth out the concentration gradients caused by these velocity fluctuations (*e.g.*, fluctuations on the scale of the particle diameter). However, this approach precludes from taking into account the large-scale fluctuations of the velocity which cause warping, undulations or other large-scale distortions of the radial shape of the band profiles which may not be smoothed out by dispersion without major loss in column efficiency, or which just subsist until elution of the zone.

In order to account for the effect of large-scale fluctuations in the bed density, we need a more sophisticated model. We assume that the velocity can be averaged out locally, over a scale large compared to the particle size, but small compared to the column radius. Since for the sake of simplicity, we assume the column to have a cylindrical symmetry, we shall consider three cylindrical distributions for the mobile phase velocity, a parabola, two parabolas with a cusp at the column center, and a cosine symmetrical around the column center (Fig. 1). These profiles are referred to later as FLOW-1 (Fig. 1a and b), FLOW-2 (Fig. 1c and d) and FLOW-3 (Fig. 1e and f), respectively. Each velocity profile is characterized by the ratio of the maximum to the minimum velocities. For each distribution, we considered the two possible cases, with either a maximum (u_M) or a minimum (u_m) of the mobile phase velocity in the column center. For each distribution, the calculations were carried out with three different ratios of the maximum to the minimum flow velocity. To permit an easy comparison of the results, the flow velocity distributions were normalized, to achieve in all cases the same value for the mobile phase flow-rate

$$F_v = \int_0^{R_c} 2\pi r u(r)\, dr \quad (8)$$

Thus, the cross-section average velocities, hence the column hold-up times, are the same for all distributions, provided the average velocity be

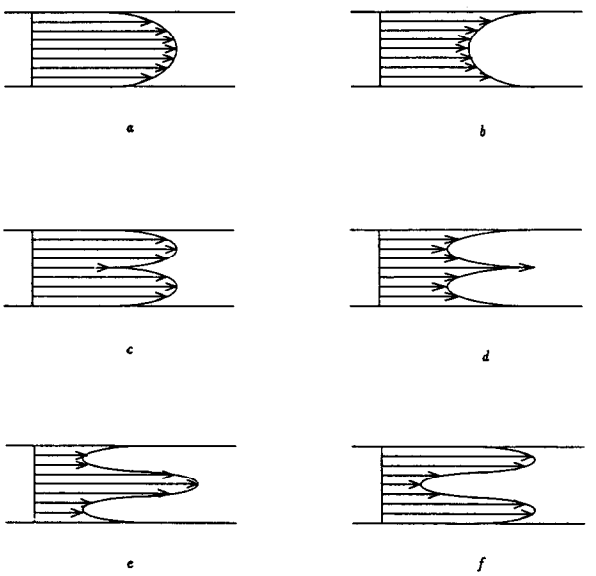

Fig. 1. Velocity distributions used for the band profile calculations (not to scale). (a) FLOW-1, parabolic distribution, $u_C > u_W$. (b) FLOW-1, parabolic distribution, $u_C < u_W$. (c) FLOW-2, cuspal distribution, $u_C < u_M$. (d) FLOW-2, cuspal distribution, $u_C > u_m$. (e) FLOW-3, cosinusoidal distribution, $u_C > u_W$. (f) FLOW-3, cosinusoidal distribution, $u_C < u_W$. u_C = Flow velocity at the column center; u_W = flow velocity along the wall.

defined from the first moment of an unretained band profile.

The velocity distributions are assumed to be fully developed and stable in each case, the velocity being constant along any parallel to the column axis. The possible contribution of transient effects at both ends of the column, where the velocity profile may be different from what it is in the column, under steady-state conditions, are neglected. Also neglected is the radial distribution of the injection profile. A piston injection profile is assumed. The effect of a radial distribution of the injection is discussed in the next section. Finally, the effect of the difference in viscosity between the pure mobile phase and the sample solution inside the moving band is also neglected. Calculations carried out in the case of an homogeneous column [17] have shown that this effect is small unless the sample concentration is very high and the viscosity of the sample is much higher than that of the mobile phase.

The parabolic distribution was chosen for its simplicity. It affords the simplest possible departure from column homogeneity. It is important to understand that the parabolic profile considered here has nothing to do with the Hagen–Poiseuille velocity profile observed in an empty tube. Although the velocity is certainly 0 at the column wall, there are no reasons for it to be smaller at a few particle diameters from the wall than at the column center, unless there is a significant gradient of packing density. In fact, as we show later, the ratio of the maximum to the minimum "local averaged" velocities as defined above which is observed in an actual preparative column is probably lower than 1.1. The other two distributions were selected because experimental results [6–9] suggest that the mobile phase velocity is indeed not constant across the column, and tends to be distributed approximately with a cylindrical symmetry, but also that the maximum velocity is located neither at the column center nor along the wall, but on a near circle having a diameter slightly larger than the column radius.

2.3. Injection profile and velocity profile

In this paper, we study the influence on the elution profile in the ideal model of a radial distribution of the velocity in the column combined with a flat injection profile. This combination is equivalent to that of a constant velocity across the entire column (flat velocity profile) with a radial distribution of the concentration at the injection, so the band profiles obtained will be similar. It is easy to prove this by comparing two experiments, one done with a column having a velocity profile, $u_0(r)$, and a flat injection profile (Fig. 2, dotted line), the other a flat velocity profile and an injection profile such that the injection pulse front shock enters into the column at time $t(r)$ and its rear shock enters the column at $t_p + t(r)$ (Fig. 2, solid line). The elution time of the front shock on the first column will be given by Eq. 6, and the retention time of the concentration C on the rear diffuse

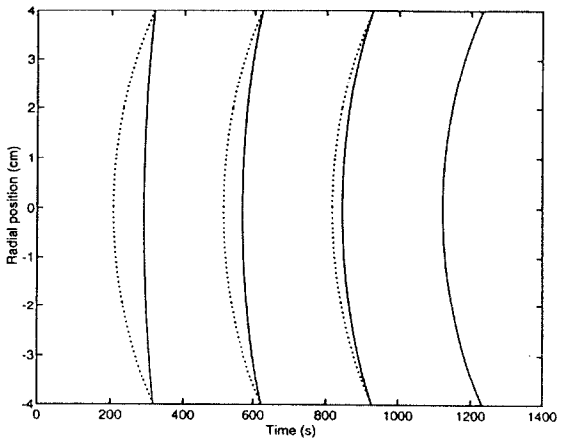

Fig. 2. Comparison between the radial distributions of the concentration obtained with a flat injection in a non-homogeneous column (solid lines) and a nonplanar injection in an homogeneous column with a flat velocity profile (dotted lines). Each profile gives the time of arrival of the front concentration shock as a function of the radial position. The different profiles correspond to different locations along the column (5, 10, 15 and 20 cm). The profile is unchanged for a non-planar injection in an homogeneous column, since there is no radial dispersion in the ideal model. The profile becomes increasing curved for a planar injection in a non-homogeneous column, because the effect of the velocity profile is cumulative.

boundary by Eq. 5b. For the second column, a similar equation can be written, giving the radial distribution of the retention time of the concentration C

$$t_R(r) = t_p + [t_0 + t(r)]\left[1 + k_0'\left(1 - \sqrt{L_f}\right)^2\right] \quad (9)$$

where $t_0 = L/u_0$ is now constant, because the velocity profile is flat (in Fig. 2) and $t(r)$ is the radial profile of the injection. The two radial and axial distributions of all the concentrations C in the elution bands on the two columns will be identical provided

$$\frac{L}{u_0} + t(r) = t_0(r) = \frac{L}{u_0(r)} \quad (9a)$$

$$t(r) = L\left[\frac{1}{u_0(r)} - \frac{1}{u_0}\right] \quad (9b)$$

Eq. 9b is the relation of equivalence between the injection profile in a column with a flat velocity profile and a column with a flat injection and a velocity profile, for them to give the same elution profile.

Accordingly, solving one problem is equivalent to solving the other one, in the framework of the ideal model, because there is no radial dispersion. The equivalence would be approximate in columns having a high efficiency, because the same combination of radial and axial dispersion coefficients would lead to different results in the two columns. Using Eq. 9b would also permit the derivation of an injection profile which would permit the calculation of a band profile affected by both a velocity distribution and an injection distribution. It could also permit the calculation of an injection distribution which would cancel the effects of a known velocity distribution, if it were practical to implement an injection with a complex injection profile.

2.4. Calculation of the elution profiles

The column is divided into n concentric annular columns of thickness $\Delta r = R_c/n$ and of radius r between 0 and R_c. In each annular column, the velocity is constant. The concentration profile at the end of each annular column is derived by applying the solution of the ideal model. The elution profile for the whole column is calculated by summing up the differential amounts eluted from all the annular columns at any given time and reporting this amount to the total volume of mobile phase in the corresponding differential slice of the column

$$\bar{C}(t) = \frac{\sum_{i=1}^{n} 2\pi r_i \Delta r\, u(r_i) C(r_i,t)}{\sum_{i=1}^{n} 2\pi r_i \Delta r\, u(r_i)} = \frac{\sum_{i=1}^{n} r_i \Delta r\, u(r_i) C(r_i,t)}{\sum_{i=1}^{n} r_i \Delta r\, u(r_i)} \quad (10)$$

where $\bar{C}(t)$ is the cross-section average concentration, r_i is the radius of the ith annular column, $u(r_i)$ is the velocity distribution and $C(r_i,t)$ is the solution of the ideal model for the ith annular column. The calculations were done with a value of n equal to 50. The chromatograms obtained are reported in the dimensionless coordinates of the Langmuir model, as $b\bar{C}$ *versus* $(t - \bar{t}_0)/$

$(t_{R,0} - \bar{t}_0)$, where $\bar{t}_0$ and $\bar{t}_{R,0}$ are the average hold-up time and the average limit retention time at infinite dilution. Both average retention times are calculated from the cross-section average mobile phase velocity. Thus, the chromatograms depend only on the velocity distribution and the loading factor.

The concentration profile given by Eq. 9 would be recorded by a detector which would mix and homogenize the entire column stream. In practice, no detector could possibly operate this way without introducing a significant amount of axial dispersion. More probably, the detector would see only part of the column effluent and give a different chromatogram depending on the exact location of the streamlet on which it operates, and one different from the actual average concentration profile. The corresponding sources of errors are not discussed in this paper.

3. Results and discussion

The calculations were carried out for two values of the loading factor, 1 and 10%. The band profiles obtained for each velocity distribution, with these two values, are presented on the same figure. The results are shown in Figs. 3–8, corresponding to the parabolic (Figs. 3 and 4), the cuspal (Figs. 5 and 6) and the cosine (Figs. 7 and 8) velocity distributions, respectively.

A quick glance at these figures shows that the band profile is very sensitive to the nature of the velocity distribution and, in each case, to the amplitude of the velocity fluctuation across the column. All the figures have a few common features, however. First, they share the angular sharpness resulting from the lack of apparent dispersion which is observed for all the profiles derived from the ideal model. Secondly, except in extreme cases, the profile remains highly unsymmetrical, with a steep front and a diffuse rear boundary. Thirdly, the influence of the velocity distribution on the band profiles is more important for the lower value of the loading factor than for the higher one. Fourthly, an important fraction of this rear boundary remains

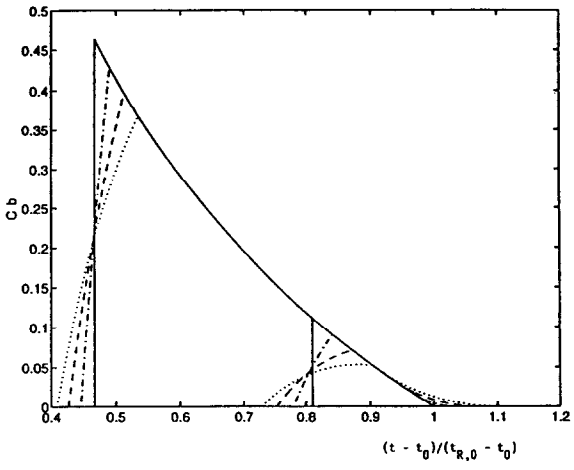

Fig. 3. Band profiles obtained with the velocity distribution in Fig. 1a. Solid line, $u_C/u_W = 1$; dashed-dotted line, $u_C/u_W = 1.05$; dashed line, $u_C/u_W = 1.10$; dotted line, $u_C/u_W = 1.15$. Right profiles, $L_f = 1.0\%$; left profiles, $L_f = 10\%$.

unchanged, whatever the velocity distribution and its amplitude. Finally, the bands end at a finite retention time, another characteristic of the ideal model and of its lack of dispersion.

Comparison of Figs. 3 and 4 (parabolic velocity distribution) shows a great similarity, indicating that, in this case, the nature of the distribution is more important than whether the

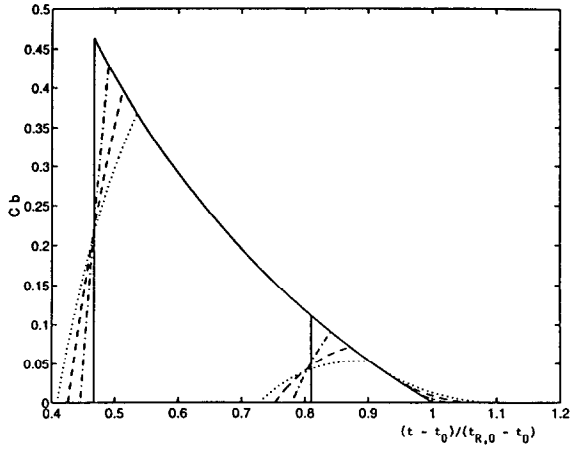

Fig. 4. Fig. 4. Band profiles obtained with the velocity distribution in Fig. 1b. Solid line, $u_W/u_C = 1$; dashed-dotted line, $u_W/u_C = 1.05$; dashed line, $u_W/u_C = 1.10$; dotted line, $u_W/u_C = 1.15$. Right profiles, $L_f = 1.0\%$; left profiles, $L_f = 10\%$.

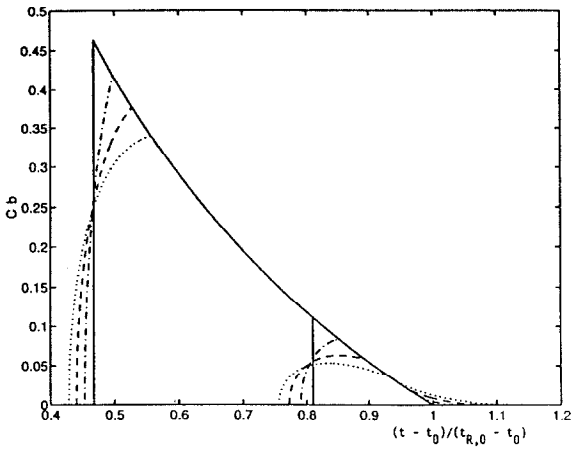

Fig. 5. Band profiles obtained with the velocity distribution in Fig. 1c. Solid line, $u_M/u_C = 1$; dashed-dotted line, $u_M/u_C = 1.05$; dashed line, $u_M/u_C = 1.10$; dotted line, $u_M/u_C = 1.15$. Right profiles, $L_f = 1.0\%$; left profiles, $L_f = 10\%$.

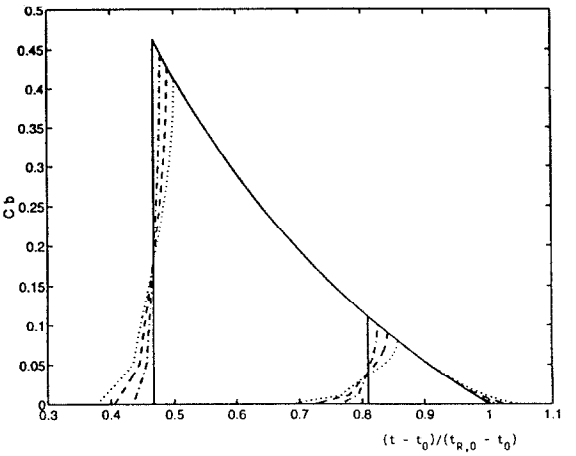

Fig. 7. Band profiles obtained with the velocity distribution in Fig. 1e. Solid line, $u_M/u_m = 1$; dashed-dotted line, $u_M/u_m = 1.05$; dashed line, $u_M/u_m = 1.10$; dotted line, $u_M/u_m = 1.15$. Right profiles, $L_f = 1.0\%$; left profiles, $L_f = 10\%$.

maximum velocity is in the center or close to the wall. For low or moderate velocity ratios, the front is slightly slanted but still nearly a straight line. The time between the beginning of the elution of the band and the elution of its maximum is nearly independent of the loading factor. Accordingly, the profiles of the small size sample bands are more strongly distorted than the heavily overloaded ones. At large velocity ratios, the front still begins as a straight line, then it curves at approximately half the height of the ideal band profile. The band tails slightly, as if the column efficiency had become finite, but still

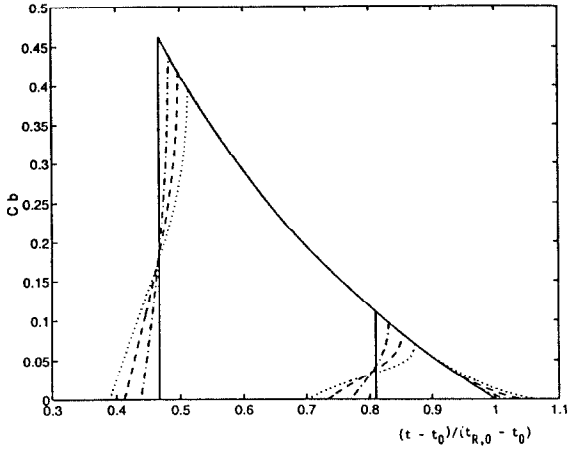

Fig. 6. Band profiles obtained with the velocity distribution in Fig. 1d. Solid line, $u_C/u_M = 1$; dashed-dotted line, $u_C/u_M = 1.05$; dashed line, $u_C/u_M = 1.10$; dotted line, $u_C/u_M = 1.15$. Right profiles, $L_f = 1.0\%$; left profiles, $L_f = 10\%$.

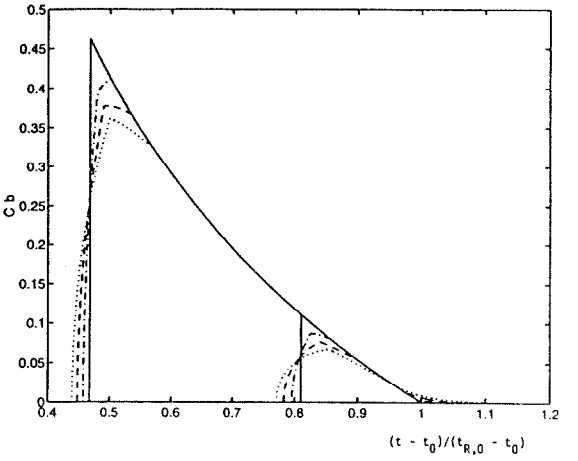

Fig. 8. Band profiles obtained with the velocity distribution in Fig. 1f. Solid line, $u_M/u_m = 1$; dashed-dotted line, $u_M/u_m = 1.05$; dashed line, $u_M/u_m = 1.10$; dotted line, $u_M/u_m = 1.15$. Right profiles, $L_f = 1.0\%$; left profiles, $L_f = 10\%$.

elution is entirely finished after a finite time. As expected [5], the rear of the band is the same for the two sample sizes.

Comparison of Figs. 5 and 6 shows a behavior significantly different from the one observed in the previous case. The band profile is strongly different depending whether the velocity is maximum at the column center (Fig. 5) or at half the column radius (Fig. 6). This is due to the fact that, by contrast with the previous case, the contributions of the different concentric regions of the column cross-section to the profile have significantly different weights. In the former case, the front begins as a shock, to turn backwards, with a slope which decreases rapidly with increasing velocity ratio. At the lower value of the loading factor, the band is nearly flat towards its maximum. The band tail is the same as for the parabolic distribution. In the latter case (Fig. 6), the band begins smoothly, and quite earlier than in the former case (Fig. 5). Beyond its half-height, the profile becomes nearly vertical. This difference is explained by the fact that the regions around the column center and the wall where the velocity is extreme has a much lower surface area than the annular region where the velocity is near its other extreme. Accordingly, the band maximum is quite sharp.

Finally, the comparison of Figs. 7 and 8 shows a situation much closer to the second case than to the first one. The main difference between Figs. 5 and 7, or Figs. 6 and 8, respectively, is in the more progressive rise of the beginning of the band front.

It is also important to observe that in all cases the band width at half-height is barely affected by the importance of the spread of the velocity distribution for a 10% loading factor. It is noticeably increased for the 1% loading factor, but even then the relative change is moderate. The baseline band width is more significantly increased. Thus, the band distortion, and especially the amount of tailing caused by a non-homogeneous packing, may have more serious effects than revealed by mere studies of band widths and apparent column efficiencies. For actual columns, the effect might not be easy to recognize unless the velocity spread is large. Radial dispersion can relax the concentration gradients arising from large-scale velocity differences over short distances. After a time t, a Dirac pulse in an homogeneous cylindrical tube becomes a Gaussian of variance $\sigma^2 = 2Dt$. Thus, the Fick number, $Fi = z^2/2Dt$, is used to characterize the extend of relaxation of a concentration gradient by dispersion. A Fick number of 1 corresponds to a distance equal to $\sqrt{2Dt}$.

In an actual chromatographic column, the radial dispersion coefficient includes contributions of the molecular and eddy diffusions similar to those involved in the axial dispersion coefficient, but does not include any contributions of the resistance to mass transfer inside the particles nor of the kinetics of adsorption/desorption [7,10]. Accordingly, D_r can be estimated to be between one half and one fifth of $D_a = HL/2t_0 = Hu/2$, depending on the mobile phase velocity (where D_a and D_r are the axial and radial dispersion coefficients, respectively). The distance over which a concentration gradient can be relaxed during the band migration is of the order of $\sqrt{HL/2}$ to $\sqrt{HL/5}$. With values of the column HETP in the 20 to 50 μm range and typical column lengths being around 20 cm, we obtain 0.14 cm, which is indeed small compared to the diameter of most preparative columns. It is barely a quarter of the diameter of conventional analytical columns. Indeed, Knox and Parcher [10] have shown that if a point-like injection is performed at the column center, the elution zone never sees the wall of a conventional column.

The worse chromatogram we have obtained so far, with a radial compression column severely mistreated by raising the inlet pressure above the compression pressure to induce the formation of cracks in the packing [18], is shown in Fig. 9. As this figure illustrates, actual overloaded elution profiles may look somewhat as predicted using a cylindrical velocity distribution (compare the profile in Fig. 9 and the high concentration profiles corresponding to a velocity ratio of 1.05 in Figs. 5 and 8). Nevertheless, in view of the profiles generated in this study, the degree of homogeneity which can be achieved when packing large-diameter preparative columns appears to be more than satisfactory. It seems to corre-

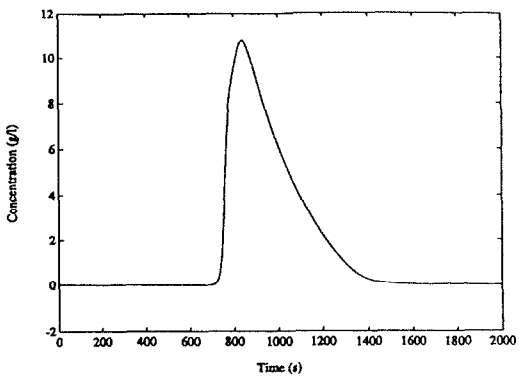

Fig. 9. Experimental band profile obtained with a worn out 17.5 × 7.5 cm radial compression column packed with IMPAQ RG1020C_{18}. Mobile phase methanol–water (40:60), 74 ml/min. Sample, 3.88 g phenol.

spond to velocity distributions where the range of velocity across the column does not exceed 5 to 10% of the average velocity.

4. Conclusions

The ideal model shows that major distortions of the band profiles arise whenever the mobile phase velocity changes significantly across the section of the column. It is rare that experimental profiles exhibit the large deformations which are associated with variations of the local velocity over the column width of the order of 10 to 15%. Thus, a comparison between the results of experiments and those of the calculations discussed in this work tends to show that actual columns are relatively homogeneous. However, the ideal model is not realistic, as we know from studies of classical, homogeneous columns. A radial velocity distribution creates a radial concentration gradient which will be relaxed to some extent by radial dispersion. The actual deformation of the band profiles caused by a non-homogeneous packing distribution will be less than predicted by the ideal model. Further work using a model taking both axial and radial dispersion into account is in progress and will be reported later.

Acknowledgements

This work has been supported in part by grant CHE-9201663 of the National Science Foundation and by the cooperative agreement between the University of Tennessee and the Oak Ridge National Laboratory. We acknowledge the continuous support of our computational effort by the University of Tennessee Computing Center.

References

[1] D. DeVault, *J. Am. Chem. Soc.*, 65 (1943) 532.
[2] E. Glueckauf, *Proc. Roy. Soc.*, A186 (1946) 35.
[3] H.-K. Rhee, R. Aris, N.R. Amundson, *Phil. Trans. Roy. Soc. (London)*, A267 (1970) 419.
[4] F. Helfferich and G. Klein, *Multicomponent Chromatography —A Theory of Interference*, Marcel Dekker, New York, 1970.
[5] G. Guiochon, S. Golshan-Shirazi and A.M. Katti, *Fundamentals of Preparative and Non-Linear Chromatography*, Academic Press, Boston, MA, 1994.
[6] J.H. Knox, G.R. Laird and P.A. Raven, *J. Chromatogr.*, 122 (1976) 129.
[7] C.H. Eon, *J. Chromatogr.*, 149 (1978) 29.
[8] R.M. Wightman, *Anal. Chem.*, 60 (1988) 2334.
[9] T. Farkas and G. Guiochon, *J. Chromatogr.*, submitted for publication.
[10] J.H. Knox and J.F. Parcher, *Anal. Chem.* 41 (1968) 1599.
[11] J.H. Knox, *J. Chromatogr. Sci.*, 15 (1977) 352.
[12] J.C. Giddings, *J. Gas Chromatogr.*, 1 (1962) 12.
[13] H. Colin, in G. Ganetsos and P.E. Barker (Editors), *Preparative and Production Scale Chromatography*, Marcel Dekker, New York, 1993, p. 11.
[14] R.M. Nicoud and M. Perrut, in G. Ganetsos and P.E. Barker (Editors), *Preparative and Production Scale Chromatography*, Marcel Dekker, New York, 1993, p. 47.
[15] J.N. Wilson, *J. Am. Chem. Soc.*, 62 (1940) 1583.
[16] R. Aris and N.R. Amundson, *Mathematical Methods in Chemical Engineering*, Vol. 2, Prentice Hall, Englewood Cliffs, NJ, 1973.
[17] A. Felinger and G. Guiochon, *Biotechnol. Progr.*, 9 (1993) 450.
[18] M. Sarker and G. Guiochon, *J. Chromatogr.*, submitted for publication.